Quantum noise of a Bose-Einstein condensate in an optical cavity, correlations, and entanglement

G. Szirmai,[1,2] D. Nagy,[1] and P. Domokos[1]

[1]*Research Institute for Solid State Physics and Optics, Hungarian Academy of Sciences, P.O. Box 49, H-1525 Budapest, Hungary*

[2]*ICFO-Institut de Ciències Fotòniques, Mediterranean Technology Park, 08860 Castelldefels (Barcelona), Spain*

(Received 12 January 2010; published 29 April 2010)

A Bose-Einstein condensate of ultracold atoms inside the field of a laser-driven optical cavity exhibits dispersive optical bistability. We describe this system by using mean-field approximation and by analyzing the correlation functions of the linearized quantum fluctuations around the mean-field solution. The entanglement and the statistics of the atom-field quadratures are given in the stationary state. It is shown that the mean-field solution, that is, the Bose-Einstein condensate, is robust against entanglement generation for most of the phase diagram.

DOI: 10.1103/PhysRevA.81.043639 PACS number(s): 03.75.Gg, 42.50.Wk, 67.85.Hj

I. INTRODUCTION

Nonlinear open systems often produce bistabilities or dynamical phase transitions. A nice example is the behavior of a Bose-Einstein condensate (BEC) in a pumped high-finesse optical cavity, where the nonlinearity is produced by the dispersive atom-light interaction [1–8]. The weak cavity pumping causes a classical electromagnetic field to build up between the mirrors. The atoms coupled dispersively to the radiation field detune the cavity according to the overlap of their spatial distribution with the mode function of the electric field. Consequently, the cavity resonance frequency can be shifted away from or toward the frequency of the pumping laser; thereby a big variation in intensity can be induced merely by the spatial redistribution of the atoms. In turn, the intensity change translates into the variation of the depth of the optical dipole potential, and so it acts back upon the atomic distribution itself. In a tiny region of the parameter settings close to the cavity resonance, two stable or metastable configurations can exist, giving rise to a dynamical phase transition.

Atom-light interaction itself is a major issue in the studies of ultracold quantum gases, being the most universal tool in accessing the properties of the system either by slowing the cloud of atoms, trapping them in classical potentials, putting obstacles in their path, or finally detecting and imaging them. Moreover, recent proposals have raised the possibility of quantum-state preparation of the atomic ensemble with the help of measuring the output photon signal of a pumped optical resonator [9–13]. The cornerstone of such a quantum-state preparation with the help of a quantum nondemolition measurement is also the mutual back-action between the atomic and photonic degrees of freedom. The study of correlations between atomic motion and light generated by atom-light interactions in an optical cavity is therefore of fundamental importance.

An important area of research on the manifestation of light-matter interaction is optomechanics, where the radiation pressure force of a single-mode Fabry-Pérot resonator is used to manipulate the center-of-mass motion of a mechanical oscillator. For a short review of optomechanical systems and their experimental realizations, see Ref. [14] and references therein. The reason for the popularity of optomechanical studies, besides experimental realizability, is that the theoretical description can be performed relatively simply, involving only the few modes of the cavity field and one mode for the motion of the mirror [15–17]. Such a paradigmatic system is an ideal playground to test correlations between light and mesoscopic objects, to understand the underlying physics, and to speculate on possible applications in quantum information processing.

In recent experiments done with ultracold bosons in optical resonators, the above concepts unify nicely [1–8]. The cavity radiation field couples to a single collective motional excitation of the Bose-condensed atomic sample. Starting the experiment with a pure Bose-Einstein condensate, other motional excitations can be safely disregarded and so a situation analogous to optomechanics can be realized, not with a movable mirror but rather with the collective motion of an ensemble of atoms. The differences between the experimental tools (manipulation and detection methods) of traditional optomechanical systems and those with ultracold gases nicely complement each other, while the theoretical description is very similar.

The aim of the present paper is to discuss correlations generated in a hybrid system of ultracold bosons and the radiation field, especially those close to the region of parameter settings where the system shows bistability and where the optomechanical simplification can be harvested. Photons leaking out of the resonator make the cavity field noisy, which infiltrates the dynamics of atomic motion [5,18,19]. In turn, quantum fluctuations of the atom field have a back-action on the photon statistics. Correlated fluctuations of the light and matter wave fields appear then, which are strongly enhanced close to the critical regime of bistability. The study of correlations is further motivated by the need to justify the basic assumption of the generally used mean-field theories [18,20–25], namely, that the atom-photon cross correlations are negligible and mean values of the light and atomic operators can be decoupled.

The paper is organized as follows. The backbone of the paper is Sec. II, where the model and the theoretical description of the system at the mean-field level is presented in great detail. Many of the elements of other theoretical models, for example, the cavity cooling of BEC excitations [21], spatial self-organization of a BEC in the cavity [22,26], and transient collective atomic recoil lasing [27,28] are recapitulated to give a full account of the mean-field dynamics of a BEC in a cavity. The aim, partially, is to reach the optomechanical model and discuss the assumptions and approximations involved

in arriving at that model. Special attention is paid to the effect of nonlinearities: (i) the nonlinearity caused by atom-light interaction, responsible for the creation of a periodic optical potential and also for an effective atom-atom collective interaction, and (ii) the nonlinearity caused by atomic s-wave collisions. In Sec. III, we present mean-field results and compare them to experimental observations, wherever applicable. Furthermore, the autocorrelations and cross correlations of the quantum fluctuations of the fields are calculated in the stationary state formed by the balance of cavity loss and vacuum noise driving. Finally, a summary is given in Sec. IV.

II. THEORETICAL DESCRIPTION OF THE SYSTEM

The system consists of a single-mode, high-finesse optical Fabry-Pérot resonator with a waist much smaller than the cavity length and a sample of dilute, ultracold bosonic atoms prepared to be Bose-Einstein condensed. The condensate is supposed to be cigar shaped along the cavity axis, with a strong transverse confinement. The radiation field inside the cavity is pumped through one of its mirrors by a laser with frequency ω_P and wavenumber $k = \omega_P/c$, where c is the speed of light. The laser frequency is far detuned from the atomic transitions, so the populations of the electronic excited states are negligible. In this limit, the atomic internal degrees of freedom are frozen, and the atom-light interaction is purely dispersive. On the other hand, the cavity frequency ω_C lies close to the pump frequency ω_P: the detuning $\Delta_C = \omega_P - \omega_C$ is comparable to κ, the latter being half of the inverse lifetime of a photon inside the cavity.

A. Hamiltonian

In the frame co-rotating with the pumping laser field, the Hamiltonian of the system can be approximated as

$$H = H_A + H_C + H_{AC} + H_{CL} + H_{\rm vac}, \tag{1a}$$

where H_A is the Hamilton operator of the ground-state atoms inside the cavity, given by

$$H_A = \int \Psi^\dagger(x)\left[\frac{-\hbar^2}{2m}\frac{d^2}{dx^2} + V_{\rm ext}(x) + \frac{g}{2}\Psi^\dagger(x)\Psi(x)\right]\Psi(x)\,dx, \tag{1b}$$

where m is the mass of the atoms, $V_{\rm ext}(x)$ is the external confining potential along the cavity axis, and g is the s-wave scattering constant in one dimension. The term H_C of the Hamiltonian describes the radiation field of the empty, single-mode cavity,

$$H_C = -\hbar\Delta_C\, a^\dagger a. \tag{1c}$$

The dispersive interaction between the cavity radiation field and the atoms in this low excitation limit is given by the ac Stark shift, or light shift:

$$H_{AC} = \hbar U_0\, a^\dagger a \int \Psi^\dagger(x)\Psi(x)\cos^2(k\,x)\,dx, \tag{1d}$$

where U_0 is the single-atom light shift, $U_0 = g_{CA}^2/\Delta_A$; the unique longitudinal mode function of the single-mode cavity is $\cos(kx)$ with wavenumber $k = \omega_P/c = 2\pi/\lambda$. The part describing the coupling of the cavity field to that of the pump laser is given by

$$H_{CL} = i\hbar(\eta^* a - \eta a^\dagger), \tag{1e}$$

where η is the strength of the driving field; the asterisk stands for complex conjugation. The last part of the Hamiltonian, $H_{\rm vac}$, describes the interaction of the cavity field with the broadband reservoir of external radiation field modes via the partially transmissive mirrors. We account for this interaction within the Markov approximation by means of introducing a loss rate 2κ and a Gaussian white noise operator $\xi(t)$ in the Heisenberg equation of motion for the field operators [29].

B. Equations of motion

The equation of motion of the photonic annihilation operator is given by

$$i\frac{d}{dt}a(t) = \left[-\Delta_C + \int \Psi^\dagger(x,t)\Psi(x,t)U(x)\,dx - i\kappa\right]a(t) + i\eta + i\xi(t), \tag{2a}$$

with $U(x) = U_0\cos^2(kx)$ the local single-atom light shift, which is a periodic function. Its period is noticeably $L = \lambda/2$, since it contains the mode function squared. The operator $\xi(t)$ describes Gaussian white noise with zero mean and with the only nonvanishing correlation

$$\langle \xi(t)\xi^\dagger(t')\rangle = 2\kappa\delta(t-t'). \tag{2b}$$

It is nicely exhibited in Eq. (2a) that the dispersive interaction between the atoms and the radiation field causes a shift in the resonator frequency proportional to the atomic density $\Psi^\dagger(x,t)\Psi(x,t)$. However, this frequency shift is an operator and couples the equations of motion of the radiation field to those of the atomic field operators in a nonlinear way. The equation of motion of the atomic field operator reads

$$i\hbar\frac{\partial}{\partial t}\Psi(x,t) = \left[-\frac{\hbar^2\Delta}{2m} + V_{\rm ext}(x) + \hbar a^\dagger(t)a(t)U(x) + g\Psi^\dagger(x,t)\Psi(x,t)\right]\Psi(x,t). \tag{2c}$$

In the atomic part of the equation of motion [Eq. (2c)], in addition to the inert trap potential $V_{\rm ext}$, the atom-light interaction creates a $\lambda/2$ periodic optical potential for the atoms, proportional to the dynamical photon number operator $a^\dagger a$.

C. Mean-field solution

To solve the coupled nonlinear operator equations (2) simultaneously is a hard task. The most convenient approximation is the mean-field approximation, when one first separates the operators into a mean value and to fluctuations around it:

$$\Psi(x,t) = \sqrt{N}\varphi(x,t) + \delta\Psi(x,t), \tag{3a}$$

$$a(t) = \alpha(t) + \delta a(t). \tag{3b}$$

The mean values are c-numbers, defined as $\varphi(x,t) = N^{-1/2}\langle\Psi(x,t)\rangle$, the so-called condensate wave function, which is normalized to unity; $\alpha(t) = \langle a(t)\rangle$ is the coherent part of the cavity field. Consequently, the fluctuations have zero mean. The time evolution of the mean values is obtained by substituting Eqs. (3) into the equations of motion (2) and neglecting all terms containing fluctuations. In this way, one arrives at a Gross-Pitaevskii-like set of equations of the coupled dynamics

$$i\frac{d}{dt}\alpha(t) = [-\Delta_C + N\langle U\rangle - i\kappa]\,\alpha(t) + i\eta, \tag{4a}$$

$$i\hbar\frac{\partial}{\partial t}\varphi(x,t) = \left[-\frac{\hbar^2\Delta}{2m} + V_{\rm ext}(x) + \hbar|\alpha(t)|^2U(x) + g\,N\,|\varphi(x,t)|^2\right]\varphi(x,t), \tag{4b}$$

with the notation $\langle U\rangle \equiv \int \varphi^*(x,t)U(x)\varphi(x,t)\,dx$.

There is a simplification of the numerical problem due to the possible separation of time scales. The time evolution of Eq. (4a) is governed by two characteristic frequencies, namely the detuning Δ_C and the photon loss rate κ. In Eq. (4b), the characteristic frequency is set by the recoil frequency $\omega_R = \hbar k^2/(2m)$. In experiments the latter frequency is usually several orders of magnitude smaller than the former ones. For example, in the experiments of Esslinger and colleagues [1,3,4], the parameters $|\Delta_C| \sim \kappa \approx 2\pi \times 1$ MHz, while the recoil frequency is about $\omega_R \approx 2\pi \times 4$ kHz. In this situation the dynamics of the resonator field relaxes very fast compared to the dynamics of the atomic motion and therefore can be considered instantaneous with respect to the relaxation of the condensate. One can assume for any given atomic configuration that the resonator field has already reached its steady-state value, which, by Eq. (4a), is

$$\alpha_{\rm ss} = \frac{i\eta}{\Delta_C - N\langle U\rangle + i\kappa}. \tag{5}$$

This steady-state mean field provides the optical potential in Eq. (4b). So in the end, one only integrates Eq. (4b), with $\alpha(t)$ adiabatically eliminated and inserted from Eq. (5), instead of the coupled Eqs. (4a) and (4b). It is worth noting that, if the time scales of the resonator field and BEC dynamics do not differ that much, some complex coupled solutions can exist [30], which need the simultaneous integration of Eqs. (4a) and (4b).

After the adiabatic elimination of the photon field α, the most direct method to numerically calculate the steady state of the BEC wave function $\varphi(x)$ is the one based on the imaginary-time propagation of Eq. (4b). In real time, the steady-state solution has the time dependence

$$\varphi(x,t) = \varphi(x)\,e^{-i\mu t/\hbar}, \tag{6}$$

with $\mu/\hbar$ the lowest frequency eigenvalue of the nonlinear problem (4b). In imaginary time, all fluctuations around the steady-state die out, since they propagate with higher frequencies in real time and consequently vanish faster in imaginary time than the steady-state solution. One just has to renormalize the solution $\varphi(x,t)$ after some finite propagation time. Note that, since all quantities on the left-hand side of Eq. (4b) are real, the condensate wave function $\varphi(x)$ can also be chosen as real. We also note at this point that, as is shown later, in the case of an effective blue detuning $\Delta_C - N\langle U\rangle > 0$, the resonator field heats the atomic motion (some excitations have positive imaginary parts) and there is no steady-state condensate wave function at all. However, due to the method of imaginary-time propagation, one can find a BEC wave function even in this case, corresponding to a dynamically unstable equilibrium situation.

D. Fluctuations around the mean-field solution

Having obtained the steady-state values of the BEC wave function and the resonator field amplitude, one can look for the fluctuations of the annihilation (and creation) operators $\delta a(t), \delta\Psi(x,t)$ **(**$\delta a^\dagger(t)$, $\delta\Psi^\dagger(x,t)$**)** in linear order. This linear stability analysis corresponds to the Bogoliubov theory of the BEC system [31] and has an analogy in optomechanics and also in other nonlinear systems, especially in hydrodynamics. Inserting the separation of the field operators (3) into Eqs. (2a) and (2c), and neglecting fluctuations higher than first order, one arrives at

$$i\frac{d}{dt}\delta a(t) = [-\Delta_C + N\langle U\rangle - i\kappa]\,\delta a(t) + N\alpha_{\rm ss}\int \varphi(x)U(x)[\delta\tilde\Psi(x,t) + \delta\tilde\Psi^\dagger(x,t)]\,dx + i\xi(t), \tag{7a}$$

$$i\hbar\frac{\partial}{\partial t}\delta\tilde\Psi(x,t) = \left[\frac{\hbar^2\Delta}{2m} + V_{\rm ext}(x) + \hbar|\alpha_{\rm ss}|^2U(x) - \mu + gN\varphi^2(x)\right]\times\delta\tilde\Psi(x,t) + \hbar U(x)\varphi(x)[\alpha_{\rm ss}^*\delta a(t) + \alpha_{\rm ss}\delta a^\dagger(t)] + gN\varphi^2(x)[\delta\tilde\Psi^\dagger(x,t) + \delta\tilde\Psi(x,t)], \tag{7b}$$

where the zero-order terms cancel, since they fulfill Eqs. (4b) and (5) with $d\alpha_{\rm ss}/dt = 0$. We have introduced $\delta\tilde\Psi(x,t) = N^{-1/2}\delta\Psi(x,t)\,e^{i\mu t/\hbar}$.

A closer look at Eqs. (7) reveals that the time evolution of the annihilation operators couple to those of the creation operators. It is a consequence of the complex nature of the photonic and particle fields. One can choose two equivalent ways to diagonalize Eqs. (7). The first way is to separate the complex quantities into real and imaginary parts and study their time evolution; this is the approach mainly used in optomechanical studies. The other way is to diagonalize the set of equations containing not just δa and $\delta\tilde\Psi$, but also their Hermitian adjoints $\delta a^\dagger$ and $\delta\tilde\Psi^\dagger$; this approach is familiar from the Bogoliubov-de Gennes theory of superfluidity.

Adopting the Bogoliubov-de Gennes way, we gather the fluctuations into the following column vector $R = (\delta a, \delta a^\dagger, \delta\tilde\Psi, \delta\tilde\Psi^\dagger)^T$, where the superscript T stands for transposition, and noises to the other column vector $Z = (\xi, \xi^\dagger, 0, 0)^T$. Equations (7) can now be cast into the closed form

$$i\frac{\partial}{\partial t}R(t) = \mathbf{M}R(t) + iZ(t), \tag{8a}$$

with

$$\mathbf{M}=\begin{bmatrix} A & 0 & N\alpha_{ss}X & N\alpha_{ss}X \\ 0 & -A^* & -N\alpha_{ss}^*X & -N\alpha_{ss}^*X \\ \alpha_{ss}^*Y(x) & \alpha_{ss}Y(x) & \hbar^{-1}[H_0+gN\varphi^2(x)] & \hbar^{-1}gN\varphi^2(x) \\ -\alpha_{ss}^*Y(x) & -\alpha_{ss}Y(x) & -\hbar^{-1}gN\varphi^2(x) & -\hbar^{-1}[H_0+gN\varphi^2(x)] \end{bmatrix}, \tag{8b}$$

$$H_0=-\frac{\hbar^2\Delta}{2m}+V_{\mathrm{ext}}(x)+\hbar|\alpha_{ss}(x)|^2U(x)-\mu+gN\varphi^2(x), \tag{8c}$$

$$Xf(x)=\int\varphi(x)U(x)f(x)\,dx, \tag{8d}$$

$$Y(x)=U(x)\varphi(x), \tag{8e}$$

$$A=-\Delta_C+N\langle U\rangle-i\kappa. \tag{8f}$$

Since δa is not independent of $\delta a^\dagger$ and similarly $\delta\tilde{\Psi}$ is not independent of $\delta\tilde{\Psi}^\dagger$, the matrix $\mathbf{M}$ has an important symmetry property. It is a consequence that the effect of the Hermitian conjugation of R can be obtained with a linear transformation $\mathbf{C}$ that swaps the first row with the second one and simultaneously the third one with the fourth, so $R^\dagger=\mathbf{C}R$. It directly follows from Eq. (8a) and from this symmetry property that

$$\mathbf{C}\cdot\mathbf{M}\cdot\mathbf{C}=-\mathbf{M}^*. \tag{9}$$

In order to study the correlations of the fluctuations, one first has to determine the time evolution of the fluctuation operators. One has to introduce quasinormal modes that diagonalize Eq. (8a) and therefore have a simple time evolution. Let us denote by $r^{(k)}$ the right eigenvectors of $\mathbf{M}$, that is,

$$\mathbf{M}\,r^{(k)}=\omega_k\,r^{(k)}, \tag{10}$$

with ω_k being the corresponding eigenvalue of $\mathbf{M}$. The fluctuation operator R can be expanded with the help of the eigenvectors (if they form a complete set)

$$R(t)=\sum_k\rho_k(t)r^{(k)}, \tag{11}$$

with ρ_k being the operator, or expansion coefficient, of the quasinormal mode k. The operator ρ_k is given by

$$\rho_k(t)=(l^{(k)},R(t)), \tag{12}$$

where $(\,\cdot\,,\,\cdot\,)$ is the Euclidean scalar product and $l^{(k)}$ is the left eigenvector of $\mathbf{M}$, defined as

$$\mathbf{M}^\dagger\,l^{(k)}=\omega_k^*\,l^{(k)}. \tag{13}$$

The left and right eigenvectors are normalized as usual: $(l^{(k)},r^{(l)})=\delta_{k,l}$. With the help of Eqs. (10) and (11), the normal modes obey the following uncoupled equation of motion:

$$i\frac{d}{dt}\rho_k(t)=\omega_k\,\rho_k(t)+i\,Q_k(t), \tag{14}$$

with the transformed noise operator $Q_k=(l^{(k)},Z)$. On integrating Eq. (14), the time dependence of the normal mode operators can be obtained:

$$\rho_k(t)=e^{-i\omega_kt}\,\rho_k(0)+\int_0^t e^{-i\omega_k(t-t')}\,Q_k(t')\,dt'. \tag{15}$$

For a dynamically stable sytem, one needs to have eigenvalues with negative imaginary parts. In this case fluctuations (the normal modes) decay to a steady state.

The symmetry property (9) has an important consequence on the spectrum of $\mathbf{M}$. Namely, if $\omega=\epsilon-i\gamma$ is an eigenvalue of $\mathbf{M}$, then $-\omega^*=-\epsilon-i\gamma$ is also an eigenvalue of $\mathbf{M}$. The modes corresponding to these eigenvalues form a pair with positive and negative energies.

There is an important issue concerning the stability of the normal modes: not all of them include the radiation components. For simplicity, assume that the external potential is even with respect to the center of the cavity. In this case, the combined external and optical potentials is also even, and parity is a symmetry of the full system. In this case the condensate wave function is also even, and the matrix $\mathbf{M}$ commutes with the parity operator. The eigenfunctions of $\mathbf{M}$ can therefore be classified by their symmetry (being odd or even). If the condensate fluctuation parts (third and fourth components) of an eigenvector $r^{(k)}$ are odd, then the result of the operator X acting on these components of $r^{(k)}$ is zero, since X contains an integration on the whole cavity axis and its kernel is even. For these modes there is no coupling term between the cavity field and the condensate part [see the first two rows of the matrix $\mathbf{M}$ in Eq. (8b)], and, since damping of the modes comes from the cavity decay, these modes remain undamped and just marginally stable. Consequently, if we want to describe the steady-state values of the correlations of fluctuations we have to omit those normal modes which do not couple to the radiation field (assuming that they are initially not populated).

E. Bloch states, the effects of *s*-wave scattering, and that of the collective coupling

For further analysis we suppose that $V_{\rm ext}(x) \equiv 0$; that is, the only potential in Eq. (2c) is the periodic optical potential induced by the resonator field. In this case the Bloch functions are good candidates for the complete set of single-particle wave functions:

$$\psi_{n,q}(x) = \mathcal{N} e^{iqx} u_{n,q}(x), \tag{16}$$

where $u_{n,q}(x)$ is a periodic function of period $\lambda/2$. Here n is the so-called band index and $q \in [0,4\pi/\lambda]$ is the quasimomentum of the particle. $\mathcal{N}$ is the constant for normalization. If we impose the Born-von Kármán boundary condition with p periods (the quantization volume is pL), then the normalization constant $\mathcal{N} = p^{-1/2}$, and the functions $u_{n,q}(x)$ are normalized to unity inside a period $L = \lambda/2$. For practical purposes, we also use plane waves as the basis of the $u_{n,q}(x)$ functions (not depending on the quasimomentum q):

$$u_{n,q}(x) = \frac{1}{\sqrt{L}} e^{ink_0 x}, \tag{17}$$

with $k_0 = 2k = 4\pi/\lambda$. [Of course, the basis Eq. (17) is suitable to express all other L-periodic functions as Fourier series.]

The field operator of the atoms is expanded as

$$\Psi(x) = \frac{1}{\sqrt{L\,p}} \sum_{n,q} b_{n,q}\, e^{i(nk_0+q)x}, \tag{18}$$

where $b_{n,q}$ is the annihilation operator of the plane-wave state $\psi_{n,q}$. Here n ranges over all integers and $q = 4\pi m/(\lambda p)$, with $m \in \{0,1,\ldots,p-1\}$.

The equation of motion of the annihilation operators $b_{n,q}$ is obtained easily from Eq. (2c), by inserting field operator (18) and using the orthogonality of the plane-wave states,

$$\begin{aligned} i\hbar \frac{d}{dt} b_{n,q} &= \frac{\hbar^2 (nk_0+q)^2}{2m} b_{n,q} + \hbar\, a^\dagger a\, U_0 \sum_{n'} L_{n,n'} b_{n'q} \\ &\quad + \frac{2g}{\lambda p} \sum_{\substack{n_1 n_2 n_3 \\ q_1 q_2 q_3}} b^\dagger_{n_1 q_1} b_{n_2 q_2} b_{n_3 q_3} \delta_{(n+n_1)k_0+(q+q_1),(n_2+n_3)k_0+(q_2+q_3)}. \end{aligned} \tag{19}$$

The first term corresponds to the kinetic energy, which is diagonal for the plane-wave states used. The matrix $L_{n,n'}$ appearing in the optical potential is a simple, tridiagonal matrix

$$L_{n,n'} = \tfrac{1}{4}[2\delta_{n,n'} + \delta_{n,n'+1} + \delta_{n,n'-1}]. \tag{20}$$

It is trivial that the kinetic energy is the lowest for $n = 0, q = 0$. The appearance of the optical potential makes the Hamiltonian nondiagonal in the plane-wave basis; however, it mixes only operators with the same quasimomentum q. Coupled plane waves can have indices n differing only by $\Delta n = \pm 1$. On the other hand, the s-wave scattering mixes operators with different n and different q momenta. The total momentum is conserved by the δ function imposing $(n + n_1 - n_2 - n_3)k_0 + (q + q_1 - q_2 - q_3) = 0$, which allows for normal scattering, when $q + q_1 = q_2 + q_3$, and $n + n_1 = n_2 + n_3$, and also for umklapp scattering processes, where the difference of the quasimomentum in the scattering is equal to a reciprocal lattice vector: $q + q_1 = q_2 + q_3 - \Delta n k_0$, and $n + n_1 = n_2 + n_3 + \Delta n$. It is useful at this point to estimate the characteristic frequency corresponding to the atom-atom s-wave scattering based on the physical parameters relevant to the experimental situation in, for example, Refs. [3,4]. The s-wave scattering length for the $|1,-1\rangle$ states of the ^{87}Rb atoms is about 5.3 nm. Assuming a particle number of $N = 6 \times 10^4$ atoms distributed in the cavity lattice of period $L = \lambda/2 = 390$ nm and the cavity egg-crate potential containing $p = 460$ valleys, corresponding to a cavity length of 180 μm, and the waist of the optical potential as $w = 25$ μm, the characteristic frequency of the s-wave interaction can be around $\omega_{\rm sw} = 4\pi\hbar a N/(Lpw^2 m) \approx 2\pi \times 4$ Hz. (Here we have neglected any external trapping potential.) This means that the characteristic energy of s-wave scattering is three orders of magnitude lower than that of the recoil energy separating the bands from each other. As a result, s-wave scattering dominantly occurs only with atoms in the same band, and umklapp processes can be neglected. When incorporating the effects of the confining parabolic optical potential in Ref. [3], the condensate density grows roughly by a factor of 100 and results in the ratio $\omega_{\rm sw}/\omega_R \sim 0.1$. In this situation, the contribution of umklapp processes is still small enough to expect that it does not significantly change the forthcoming results.

The mean-field equation for the condensate is obtained by the substitution

$$b_{n,q} = \sqrt{N}\delta_{q,0}\beta_n(t) + \delta b_{n,q}(t), \tag{21}$$

where β_n is the mean value of the annihilation operators. The $\delta_{q,0}$ condition for the mean field comes from the fact that the ground state of the translationally invariant system is also invariant under discrete translation; that is, the condensate wave function is periodic also with $L = \lambda/2$. [None of the terms in Eq. (21) violates the discrete translation of the system, and having $q \neq 0$ would cost in kinetic energy.] The mean-field equation then reads

$$\begin{aligned} i\hbar \frac{d}{dt}\beta_n(t) &= \frac{\hbar^2 n^2 k_0^2}{2m}\beta_n(t) + \hbar|\alpha_{\rm ss}|^2 U_0 \sum_{n'} L_{n,n'}\beta_{n'}(t) \\ &\quad + \frac{2g}{\lambda p} \sum_{n_1 n_2 n_3} \beta^*_{n_1}(t)\beta_{n_2}(t)\beta_{n_3}(t)\delta_{n+n_1,n_2+n_3}, \end{aligned} \tag{22}$$

with $\alpha_{\rm ss}$ given by Eq. (5), but now with

$$\langle U \rangle = U_0 \sum_{n,n'} \beta^*_n(t) L_{n,n'} \beta_{n'}(t). \tag{23}$$

The steady-state components of the condensate amplitudes $\beta_n(t)$ evolve as

$$\beta_n(t) = \beta_n\, e^{-i\mu t/\hbar}, \tag{24}$$

where μ is the chemical potential. It can be seen from Eq. (22) that β_n can also be chosen real for all n. Since $L_{n,n'} = L_{-n,-n'}$, and due to the symmetry of Eq. (22), it follows that $\beta_n = \beta_{-n}$, which means that the Fourier expansion of the condensate wave function contains only cosine terms.

The equation of motion for the fluctuations, in this representation, is given by

$$i\frac{d}{dt}\delta a(t) = [-\Delta_C + N\langle U\rangle - i\kappa]\,\delta a(t) + NU_0\alpha_{\rm ss}\sum_{n,n'}\beta_n L_{n,n'}(\delta\tilde{b}_{n',0} + \delta\tilde{b}^{\dagger}_{-n',0}) + i\xi(t), \tag{25a}$$

$$i\hbar\frac{d}{dt}\delta\tilde{b}_{n,q} = (H_0)_{n,n'}\,\delta\tilde{b}_{n',q} + \hbar U_0\delta_{q,0}(\alpha^*_{\rm ss}\delta a + \alpha_{\rm ss}\delta a^{\dagger})\sum_{n'}L_{n,n'}\beta_{n'} + \frac{2g}{\lambda p}\sum_{n_1,n_2,n'}\beta_{n_1}\beta_{n_2}(\delta\tilde{b}_{n',q} + \delta\tilde{b}^{\dagger}_{-n',-q})\delta_{n+n_1,n'+n_2}, \tag{25b}$$

with

$$(H_0)_{n,n'} = \frac{\hbar^2(nk_0+q)^2}{2m}\delta_{n,n'} + \hbar|\alpha_{\rm ss}|^2U_0L_{n,n'} + \frac{gN}{Lp}\sum_{n_1,n_2}\beta_{n_1}\beta_{n_2}\delta_{n+n_1,n'+n_2} - \mu\delta_{n,n'}. \tag{25c}$$

For a qualitative understanding of Eqs. (25), let us consider first the weak photon-atom coupling case, when either the photon number inside the cavity is small or U_0 is small. In this situation, the atomic distribution is essentially unmodified by the periodic potential and the condensate wave function is almost homogeneous (i.e., $\beta_n = \delta_{n,0}\beta_0$). Fluctuations in the atomic density are induced from the homogeneous condensate. In linear order, the atom-light interaction excites fluctuations to bands $n \pm 1$ with $q = 0$, while the s-wave interaction populates fluctuations with arbitrary n and q. However, as discussed earlier, in the limit $\omega_{\rm sw} \ll \omega_R$, s-wave scattering induces essentially only intraband transitions; therefore, for a homogeneous condensate, only states with $n = 0$ are populated by s-wave interactions. Figure 1 depicts graphically the population of fluctuations excited from the homogeneous condensate wave function in leading order. Moreover, in experiments [3,4], the one atom light shift is a tunable parameter; its typical value is chosen to be on the order of the recoil frequency (i.e., $U_0 \approx 2\pi \times 4$ kHz) and is also much larger than the characteristic frequency of s-wave scattering. Therefore, on the time scale in which the steady state is reached, the effect of s-wave scattering is still not significant. When describing the steady state, one can safely neglect it as a first approximation and consider each band represented by a single-state vector with $q = 0$.

Note that there is an interesting complementary regime in which the relevant states are localized, Wannier-type states formed by the coherent superposition of many quasimomentum states with $q \neq 0$. To describe many-body effects of the atomic degree of freedom in this regime, one can resort to a Bose-Hubbard model with self-consistent parameters [32–37], in which collisions play a vital role but interband transitions are usually neglected.

F. Optomechanics

In the experimental situation of Refs. [3,4], the BEC wave function can be considered almost homogeneous, with a condensate fraction in the β_0 state containing 6×10^4 atoms,

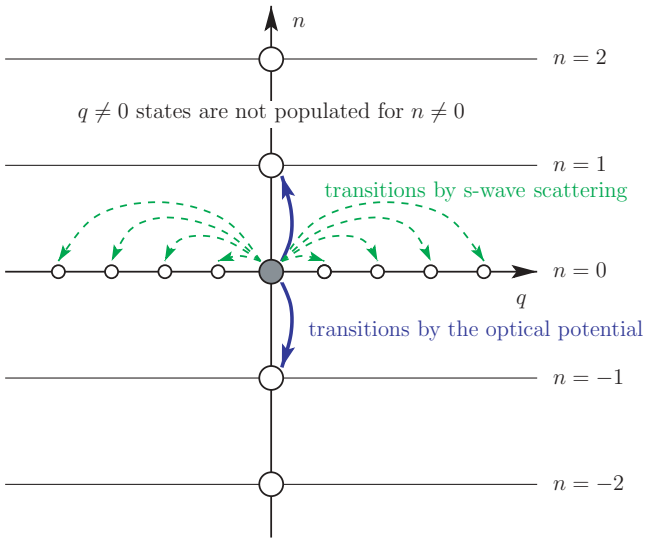

FIG. 1. (Color online) Schematic diagram of fluctuations coupling to the the homogeneous BEC in linear order. The gray circle represents the macroscopically occupied (BEC) state, while the open circles represent states which are not macroscopically occupied. The arrows show how these states can be populated in linear order by scattering from the condensate via the interaction with the photon field and also via the s-wave scattering.

while the next state with $n = \pm 1$ (i.e., the atomic motional state with wave function $\cos k_0 x$) contains only a few hundred atoms. Let us therefore restrict the Hilbert space of the one-particle atomic motion into this relevant two-dimensional subspace, containing the homogeneous single-particle wave function and that of $\cos k_0 x$. The atomic field operator becomes

$$\Psi(x) = \varphi_0(x)b_0 + \varphi_1(x)b_1, \tag{26}$$

with the single-particle wave functions $\varphi_0(x) = L^{-1/2}$ and $\varphi_1(x) = \sqrt{2/L}\cos(k_0 x)$, and their corresponding annihilation operators b_0 and b_1. The single-particle wave function $\sin(k_0 x)$, corresponding to the antisymmetric combination of the $n = \pm 1$ states, is omitted, since this wave function does not couple to the photonic field due to symmetry reasons mentioned above.

In this model the atomic motion is represented in a two-mode Fock space. The mean field expansion is

$$b_n = \sqrt{N}\beta_n + \delta b_n, \quad n = 0,1, \tag{27}$$

where β_n is again the representation of the condensate wave function in the two-dimensional Hilbert space, normalized to unity. The presence of a Bose-Einstein condensate distinguishes a subspace of one single mode. Accordingly, the fluctuation operators can be expanded to a part parallel to the condensate and to one orthogonal to it:

$$\delta b_n = \beta_n\delta b + \gamma_n\delta c, \tag{28}$$

where γ_n is the unit vector orthogonal to the condensate, $\gamma_n = (-\beta_1, \beta_0)^T$. The part, δb, parallel to the condensate can be related to the arbitrariness of the phase of the condensate and corresponds to a zero mode. The orthogonal part, δc, is the sole degree of freedom. Therefore, the fluctuations of the

atomic field, similarly to the photon field, have a single degree of freedom. The fluctuations of the combined atom-resonator field system have two degrees of freedom, and are analogous in many ways to cavities with a moving mirror, to the so-called optomechanical systems.

In order to obtain the mean-field equations and the fluctuation equations in linear order, one can start from Eq. (2) and use the truncated field operator (26) and then the mean-field ansatz (27). The mean-field equations for the condensate now read

$$i\frac{d}{dt}\beta_k(t) = [4\,\omega_R(P_1)_{k,l} + |\alpha_{\rm ss}|^2 U_{k,l}]\beta_l(t), \tag{29}$$

with $P_1 = \mathrm{diag}(0,1)$, the projection matrix to the subspace of $\varphi_1(x)$; the matrix representing the light shift is given by

$$U_{k,l} = \langle\varphi_k|U(x)|\varphi_l\rangle = \frac{U_0}{2}\begin{bmatrix} 1 & \sqrt{2}/2 \\ \sqrt{2}/2 & 1 \end{bmatrix} \tag{30}$$

and $\alpha_{\rm ss}$ is given by Eq. (5), with $\langle U\rangle = \beta_k^*(t)U_{k,l}\beta_l(t)$. (Note the convention of automatic summation over repeated indices.) The condensate wave function also has the time dependence of Eq. (24), with β_k chosen real. Equation (29) can also be solved either by imaginary-time propagation or by direct algebraic means using Eq. (24) and the normalization condition: $\beta_0^2 + \beta_1^2 = 1$.

The equations of motion for the fluctuation operators can be derived in a way analogous to how Eqs. (25) were obtained. It is appropriate to separate the trivial time dependence due to the chemical potential via the definition $\delta\tilde{b}_k = N^{-1/2}\,e^{i\mu t/\hbar}\,\delta b_k$. With this,

$$i\frac{d}{dt}\delta\tilde{a} = (-\delta - i\kappa)\delta a + N\alpha_{\rm ss}\beta_k U_{k,l}(\delta\tilde{b}_l + \delta\tilde{b}_l^\dagger), \tag{31a}$$

$$i\frac{d}{dt}\delta\tilde{b}_k = K_{k,l}\delta\tilde{b}_l + (\alpha_{\rm ss}^*\delta a + \alpha_{\rm ss}\delta a^\dagger)U_{k,l}\beta_l, \tag{31b}$$

with $\delta = \Delta_C - N\langle U\rangle$, and

$$K_{k,l} = 4\omega_R(P_1)_{k,l} - \frac{\mu}{\hbar}\delta_{k,l} + |\alpha_{\rm ss}|^2 U_{k,l}. \tag{31c}$$

The matrix K can be thought of being the grand canonical Hamiltonian of the system, and by virtue of Eqs. (29) and (24), $K_{k,l}\,\beta_l = 0$. Equations (31a) and (31b) form a linear eigenvalue problem for the fluctuations. It is easy to check that the trial function of $\delta a = 0$ and $\delta\tilde{b}_k = \beta_k\delta\tilde{b}$ is a constant solution (i.e., it is a zero mode). It also follows from the normalization of β_k that $\delta\tilde{b}$ is anti-Hermitian. With the decomposition $\delta\tilde{b}_k = \beta_k\,\delta\tilde{b} + \gamma_k\,\delta\tilde{c}$, one can arrive at a closed set of equations between the fluctuations δa and $\delta\tilde{c}$ and their Hermitian adjoints:

$$i\frac{d}{dt}\delta\tilde{a} = (-\delta - i\kappa)\delta a + N\alpha_{\rm ss}(\beta_k U_{k,l}\gamma_l)(\delta\tilde{c} + \delta\tilde{c}^\dagger), \tag{32a}$$

$$i\frac{d}{dt}\delta\tilde{c} = (\gamma_k K_{k,l}\gamma_l)\,\delta\tilde{c} + (\gamma_k U_{k,l}\beta_l)(\alpha_{\rm ss}^*\delta a + \alpha_{\rm ss}\delta a^\dagger). \tag{32b}$$

Note that, in the optomechanical model, s-wave scattering cannot be included in general because it populates states with $q \neq 0$, which are disregarded in this model. It is possible to include some remaining effects of the atom-atom collision by coupling only the two states under consideration; however, this approach would result in a nonlocal and unphysical interaction in coordinate space. Or, in order to extend the optomechanical model, although still lacking the full consideration of s-wave scattering explicitly, the higher quasimomentum states can be taken into account either by considering a (close to, but non-) plane-wave condensate wave function [25] or by using a two-fluid model [38].

III. RESULTS

In the following we summarize and discuss our results based on the numerical solutions of Eqs. (4) and (7) and compare them with those of Eqs. (29) and (32) and to the findings of Esslinger and colleagues [3,4].

A. The mean-field solution

For a comparison between the full Gross-Pitaevskii equation (GPE) solution and the optomechanical model, we numerically solve the Gross-Pitaevskii equation (4b) on a 200-point grid with imaginary-time propagation with the steady-state value of the mean radiation field amplitude (5) and compare it to the solution of Eq. (29) (also in imaginary time). The results for the mean photon number are plotted in Fig. 2. The bistable behavior is nicely exhibited in these figures. In Fig. 2(a), the pumping strength $\eta = 80.06\,\omega_R$ is below a threshold value, and the resonance curve gives a unique solution for all detunings Δ_C. Notice that, in Eq. (4a) or Eq. (5), the effective detuning of the resonator field is $\delta = \Delta_C - N\langle U\rangle$; that is, the light shift further detunes the cavity. On the left side of the resonance, the effective detuning δ is negative, and the cavity is detuned to the red. We see in the next subsection that this situation corresponds to cavity cooling, where the imaginary part of the fluctuation spectrum of the combined atom-photon system is negative (or nonpositive for the many-mode system). Fluctuations decay to zero. On the right side of the resonance, where δ is positive, the imaginary part of the fluctuation spectrum changes its sign. Fluctuations grow exponentially on this side of the resonance; that is, the slightly retarded cavity field dynamics heats the atomic motion instead of cooling it. Therefore, the solution above the resonance ($\delta > 0$) is dynamically unstable. It is only due to the adiabatic elimination of the photon field that the numerical method finds this solution as well. Note that the parameters of our calculations mimic those of Ref. [4]. The agreement in the photon number with Fig. 3 of Ref. [4] is well within the systematic uncertainty of the photon number estimation of the experiments (25%). With the use of the recoil frequency for rubidium atoms, $\omega_R = 2\pi \times 3.57$ kHz, we can compare the location of the resonance points to the experimental findings, too. In Fig. 2(a), the resonance point is at around $28\,800\ \omega_R \approx 2\pi \times 103$ MHz; in Fig. 2(b), the two instability points are at around $26\,700\omega_R \approx 2\pi \times 95$ MHz and $27\,700\ \omega_R \approx 2\pi \times 99$ MHz. All these are within 5% of the respective experimental value. In Fig. 2(c), the resonance points are at around $21\,500\omega_R \approx 2\pi \times 77$ MHz and $27\,000\omega_R \approx 2\pi \times 96$ MHz. This latter value is only 2% higher than in the experiment, but the lower point is contrasted to the $2\pi \times 84$ MHz value (about 10% deviation). In our case the bistable region is a bit wider than in the experiments. This discrepancy might be attributed mainly to the uncertainty in the effective detuning δ, which we obtain by an estimation

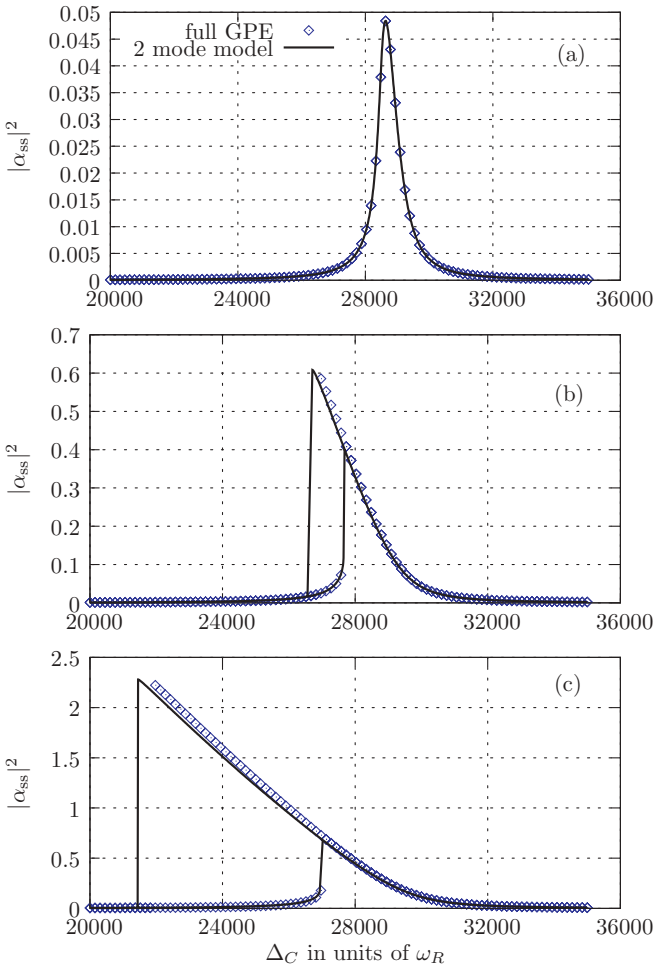

FIG. 2. (Color online) The mean cavity photon number $|\alpha_{ss}|^2$ as a function of the cavity detuning Δ_C. The parameters are $N = 6 \times 10^4$, $U_0 = 0.96\,\omega_R$, and $\kappa = 363.9\,\omega_R$. The pumping strength is different for the three panels: $\eta = (80.06, 283.8, 549.5)\omega_R$ for panels (a), (b), and (c), respectively.

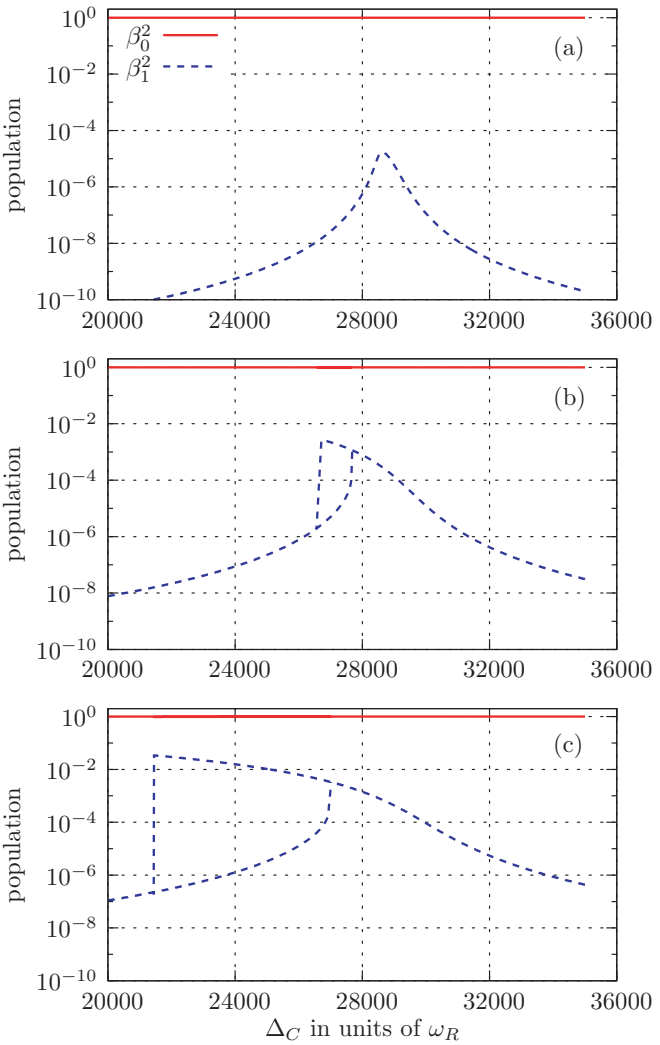

FIG. 3. (Color online) The squares of the condensate components β_0^2 and β_1^2 as a function of the detuning Δ_C in a semilog scale. The parameter settings are the same as for Fig. 2.

of the actual atom number and overlap between the cavity potential and the atomic cloud.

For $\eta > \eta_c(\Delta_C, \kappa, U_0, N)$, the threshold value of the pumping strength depending on the detuning, the cavity loss, the light shift, and also the atom number, there is a region where three solutions exist for the photon number and also for the condensate wave function. Two of them are stable solutions for the numerical method we use. These solutions are plotted in Figs. 2(b) and 2(c) for $\eta = 283.8\,\omega_R$ and $\eta = 549.5\,\omega_R$, respectively. The unstable solution is not plotted in the figure. We note, however, that the upper one of the two plotted solutions corresponds to the $\delta > 0$, cavity-heating, situation. So this solution is also unstable dynamically. But since this instability is related to photon dynamics (neglected at this level), one can still find this solution by integrating the GPE for the atoms in imaginary time.

The fraction of condensate atoms occupying the homogeneous and the $\cos k_0 x$ states are plotted on Fig. 3. The parameter settings are the same as for Fig. 2. Both the resonance feature and the bistability is exhibited in the condensate component of the $\cos k_0 x$ mode. The condensate is almost homogeneous for the whole range, $\beta_1^2 \ll \beta_0^2 \approx 1$, and β_1^2 shows a very similar dependence as the photon number. It is remarkable that a very small change in the shape of the condensate wave function causes a drastic increase or decrease of the photon number. This can be elucidated by the collective coupling of the atoms to the resonator field. The detuning $\delta = \Delta_C - N\langle U \rangle$, appearing in the denominator of the steady-state value of the resonator field (5), can change a lot even if the variation of $\langle U \rangle$ is small, because of the large number N multiplying it.

B. Fluctuation spectrum

The linear stability analysis of the mean-field solution is done with the help of linear equations (7) for the case of the full model, and with the help of Eqs. (32) for the optomechanical approximation. Once the condensate wave function and the steady-state value of the mean cavity field are known, one can construct the matrix **M** and calculate its eigenvalues and eigenvectors. In the full model, discretized on a grid with 200 sites, **M** is a 402×402 matrix, since it acts on a row

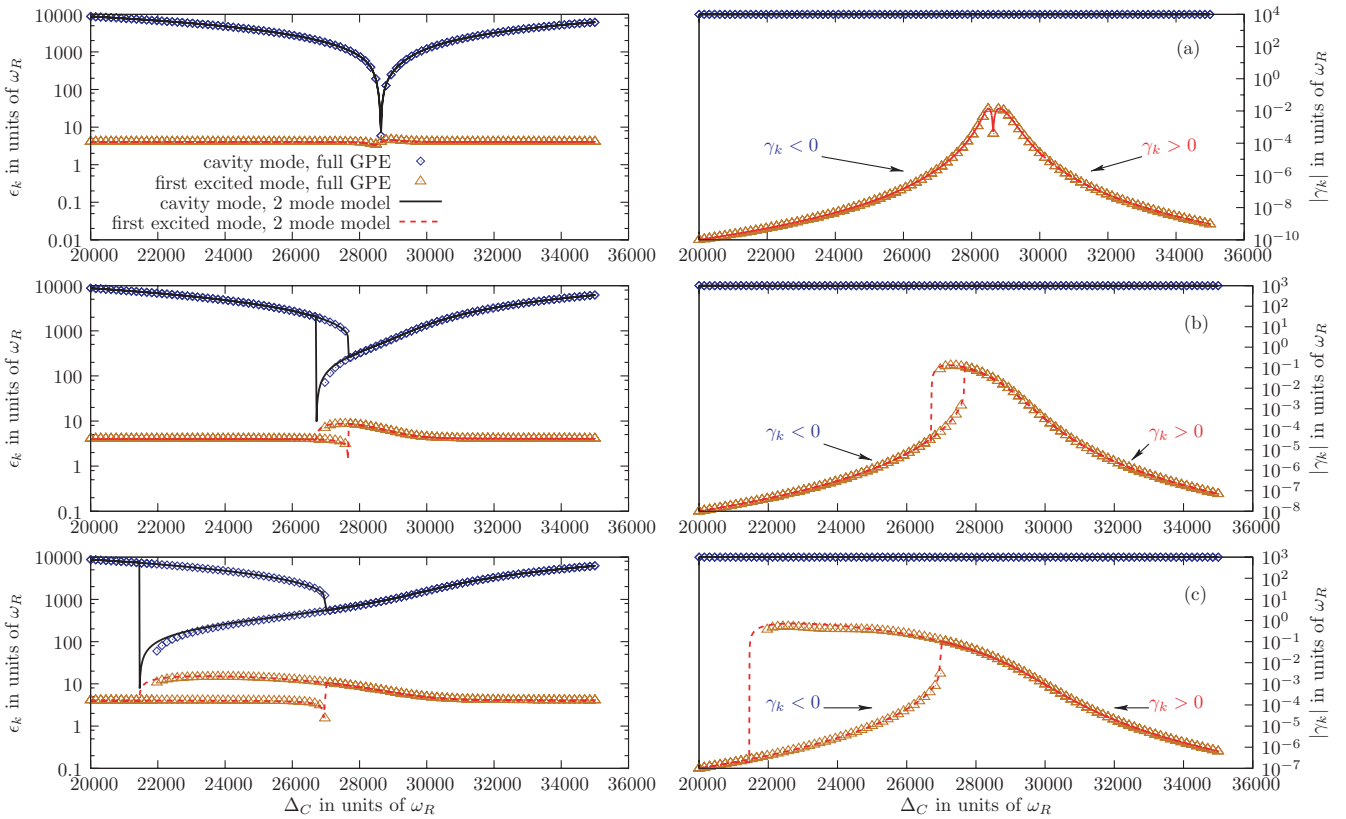

FIG. 4. (Color online) The fluctuation spectrum $\omega_k = \epsilon_k + i\gamma_k$ of the atom-cavity dynamics. The real and imaginary parts of the eigenvalues are plotted as functions of Δ_C. All quantities are measured in units of the recoil frequency. The parameter settings are the same as for Fig. 2. Note that the fluctuation spectrum of the full model, discretized on a 200-point grid, contains 201 pairs of eigenvalues. We only plot the two which correspond to those of the optomechanical system.

vector that has 2 elements for the photon fluctuation operator and its Hermitian adjoint, and also has 400 elements for the discretized field fluctuation operator and on its Hermitian adjoint. For the optomechanical model, one has a much smaller (4×4) matrix, since the zero mode is already separated in this case, so one has two components for the photon fluctuations and two components for the atomic motion orthogonal to the condensate wave function. The numerical diagonalization was obtained with the help of the LAPACK package.

Note that **M** is a general complex matrix. Its eigenvalues are complex. However, due to symmetry relation (9), the eigenvalues of **M** come in pairs. Each element of the pair has the same imaginary part, while the real parts are just the opposite of each other. Figure 4 shows the eigenvalues of **M** for the same parameter settings as that of Figs. 2 and 3. The left panels show the real part ϵ_k of the kth eigenvalue, while the right panels show the modulus of the imaginary parts γ_k for $\omega_k = \epsilon_k + i\gamma_k$. Only those two eigenvalues are plotted, which are present in the optomechanical model and have positive real parts. The other two eigenvalues of the optomechanical model can be obtained simply by changing the sign of the real parts to negative: $\omega_k \to -\epsilon_k + i\gamma_k$. In the bistability regime, the excitation frequencies are presented for both mean-field solutions.

Again, all figures show that the optomechanical approximation very well reproduces the results of the full GPE simulation even for dynamical quantities. The two modes are easy to be physically interpreted. The first eigenvalue, having a bigger real part around $\delta = \Delta_C - N\langle U\rangle$ and an imaginary part almost exactly at $-\kappa$, corresponds mainly to a photonic mode. Note that the imaginary part of this mode also remains negative above the resonance. The other eigenvalue, having a real part around $4\,\omega_R$, corresponds mainly to atomic fluctuations. The imaginary part of this eigenvalue changes sign at resonance. Below resonance, the imaginary part is negative (fluctuations in the atomic motion are damped due to the interaction with the resonator field [39,40]), while above resonance the imaginary part becomes positive (fluctuations in the atomic motion are exponentially growing in time). The situation is clear in Fig. 4(a), where the resonance point can be exactly defined. In Figs. 4(b) and 4(c), the coexistence of the two solutions makes the definition of the resonance point ambiguous. Nevertheless, in Figs. 4(b) and 4(c), the curves which continue to the left-hand side of the figure correspond to the solutions with cavity cooling, and those which continue to the right-hand side correspond to the heating solution. The dynamical cooling and heating effects are closely related to the same effects at the single-atom level [41–45].

In Refs. [3,4], the coherent atomic dynamics was also studied. The harmonic oscillator behavior of the low-energy atomic dynamics caused periodic oscillations in the output photon signal with a frequency close to 35 kHz, as reported and explained in Ref. [3], or close to around 42 kHz in Ref. [4]. In our model, the dynamics of the two coupled harmonic

oscillators of the resonator field and the atomic collective motion is described by Eqs. (32). These are linearized equations of motion around the steady-state configurations. For very small fluctuations, the semiclassical time evolution can be interpreted as orbitals around the steady-state fixed points with frequencies plotted in the left panels of Fig. 4. Due to the imaginary parts, the trajectories spiral closer to (for fluctuations around the cooling solution) or farther from (for fluctuations around the heating solution) the corresponding fixed point. From Fig. 4 we can see that the frequency of fluctuations dominated by atomic motion is close to $4\,\omega_R$ for parameters not very close to the bistable region. In the bistable regime, two steady-state solutions exist, and correspondingly there are two fixed points in the harmonic oscillator phase space. According to Fig. 4, the oscillation frequency for the cooling fixed point remains around $4\,\omega_R$ and softens close to the endpoint, while for the heating solution the oscillation frequency grows to around $10\,\omega_R$ before softening at its endpoint. This kind of renormalization of the atomic dynamics by the interaction with radiation is often referred to as the "optical spring effect." The approximately $10\,\omega_R$ angular frequency quantitatively gives back the experimentally found 42-kHz oscillation frequency of the Fig. 3C inset of Ref. [4].

It is interesting to point out that in the bistable region even small atomic fluctuations can result in a phase-space trajectory that orbits around both of the fixed points (see Fig. 3 of Ref. [3]). In this case, such a linearization strategy simply cannot work because the transition between the two fixed points is necessarily a nonlinear effect. However, if the trajectory were to lie in the basin of the linear region of the corresponding fixed points everywhere except the small region of the separatrix, one could expect the oscillation to be described by the above two frequencies: when the system is in a part of the trajectory inside the attraction basin of the cooling fixed point, the angular frequency would be around $4\,\omega_R$, while after crossing the separatrix it would change to around $10\,\omega_R$. Such a trajectory of coherent oscillations would also cause a periodic output photon signal but both of the frequencies would appear (i.e., the count rate peaks would come in pairs).

Figure 5 depicts the regions in the parameter space which represent the heating (cooling) solutions, that is, the solutions with dynamical instability (stability). The bistable region, where both a heating and a cooling solution can be found, is wedged between the two distinct regions. The tip of the wedge corresponds to the critical point (Δ_{Cc},η_c).

C. Correlations and entanglement

Second-order correlations of the fluctuations are calculated with the help of the quasinormal modes and the noise correlations, since by virtue of Eqs. (11) and (15)

$$\begin{aligned}\langle R_k(t)\,R_l(t)\rangle &= \sum_{m,n}\langle \rho_m(t)\,\rho_n(t)\rangle\, r_k^{(m)}\, r_l^{(n)} \\ &= \sum_{m,n} r_k^{(m)}\, r_l^{(n)}\Big[e^{-i(\omega_m+\omega_n)t}\langle \rho_m(0)\,\rho_n(0)\rangle \\ &\quad + \int_0^t dt_1 dt_2 e^{-i\omega_m(t-t_1)} e^{-i\omega_n(t-t_2)}\langle Q_m(t_1) Q_n(t_2)\rangle\Big]. \end{aligned} \tag{33}$$

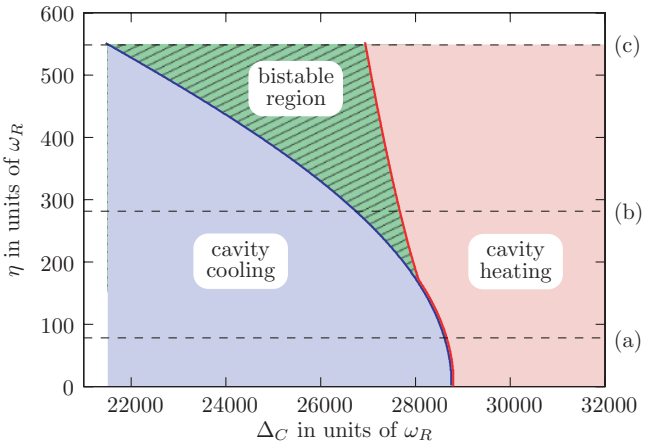

FIG. 5. (Color online) The nonequilibrium phase diagram of the system indicating the parameter regions with full dynamical stability (the cooling region) and the region with a dynamical instability caused by the energy transfer of the cavity (the heating region). The horizontal lines represent the parameter η at values corresponding to panels (a), (b), and (c) of other figures with numeric results.

For a stable system, where all the eigenvalues have negative imaginary parts, the first term on the right-hand side, corresponding to the initial condition of the fluctuations, vanishes for times much longer than the characteristic decay times of the system. For the second term, one can use the noise correlation function (2b), and the definitions of the vector noise Z and that of Q. For $t\to\infty$, it follows straightforwardly that

$$\langle R_k(t)\,R_l(t)\rangle \to 2\kappa \sum_{m,n} \frac{l_1^{(m)*}\, l_2^{(n)*}\, r_k^{(m)}\, r_l^{(n)}}{i(\omega_m+\omega_n)}, \tag{34}$$

where we index the components of the row vectors R and Z starting from 1, and also drop the exponential term vanishing for large times in the case of a stable system. Note that the zero mode [i.e., δb in Eq. (28)], representing the phase fluctuations of the condensate, does not contribute to this sum because its eigenfunction does not have photon component; that is, $l_1^{(\text{zero mode})} = l_2^{(\text{zero mode})} = 0$.

To be able to relate our results more explicitly to other works, let us introduce quadrature operators, according to $\delta x = (\delta a + \delta a^\dagger)/\sqrt{2}$, $\delta y = -i(\delta a - \delta a^\dagger)/\sqrt{2}$, $\delta X = (\delta c + \delta c^\dagger)/\sqrt{2}$, and $\delta Y = -i(\delta c - \delta c^\dagger)/\sqrt{2}$. These quadrature operators are Hermitian operators and are easily expressed with the help of the field operators R. We assemble them into the following row vector: $u = (\delta x,\delta y,\delta X,\delta Y)^T$. With the quadratures being Hermitian, one can define a real correlation matrix by

$$C_{k,l}(t) = \tfrac{1}{2}\langle u_k(t)\,u_l(t) + u_l(t)\,u_k(t)\rangle, \tag{35}$$

which is in the following block form,

$$\mathbf{C} = \begin{bmatrix} \mathbf{P} & \mathbf{X} \\ \mathbf{X}^T & \mathbf{A} \end{bmatrix}, \tag{36}$$

where $\mathbf{P}$ represents the correlations of the photonic degree of freedom, $\mathbf{A}$ represents atomic fluctuations, and $\mathbf{X}$ describes the cross correlations. For example, on top of the mean-field

contribution $|\alpha|^2$, there is a nonclassical part of the photon number which is given by

$$n'_{\rm ph} = \langle \delta a^\dagger \, \delta a \rangle = \frac{\langle \delta x^2 \rangle + \langle \delta y^2 \rangle - 1}{2} = \frac{C_{1,1} + C_{2,2} - 1}{2}. \tag{37}$$

In an empty resonator close to zero temperature, where $\langle \xi^\dagger(t) \xi(t') \rangle = 0$, the nonclassical part of the photon number [Eq. (37)] vanishes, and the resonator field is in a pure coherent state. The fluctuations of the quadratures are distributed equally and the Heisenberg uncertainty principle is fulfilled in a sharp sense ($\langle \delta x^2 \rangle = \langle \delta y^2 \rangle = 1/2$). However, due to atom-photon interaction, the photon fluctuations couple to those of the atomic motion. By iterative substitution of Eqs. (32), one can simply check that $n'_{\rm ph} = \langle \delta a^\dagger \delta a \rangle$ is no longer zero in the presence of a Bose-Einstein condensate. The photon field is no longer in a purely coherent state, and the correlation matrix **P** is not simply half of the unit matrix. Indeed, since δa couples now to $\delta a^\dagger$ (through $\delta \tilde{c}$) and the coupling term is proportional to $\alpha_{\rm ss}^2$, which is complex, the correlation matrix **P** is not isotropic. The angle of the major axis coincides with twice the phase of $\alpha_{\rm ss}$, taking the values from $-\pi$ (when the system is far from the resonance) to zero (at resonance). By performing a rotation of the correlation matrix by this angle to bring it into a diagonal form, one of the eigenvalues will remain $1/2$, as in the pure coherent-state case, while the other one will always become bigger than $1/2$. Since the trace of a matrix is invariant under rotations, the nonclassical part of the photon number $n'_{\rm ph} = (\lambda_> - 1/2)/2$, where $\lambda_>$ is the bigger eigenvalue of **P**. Figure 6 shows the nonclassical contribution to the photon number. The classical average $|\alpha_{\rm ss}|$ of Fig. 2 is also plotted with a dashed line for reference. It can be seen, by comparing the two curves, that the nonclassical contribution to the photon number is very small compared to the contribution of the mean field far from the resonance. When approaching the resonance, the nonclassical part grows faster than the mean-field part, and, in the vicinity of the resonance, it even exceeds the mean-field contribution. The nonclassical contribution of the photon number is plotted only for the cavity cooling regime, where a steady-state solution exists.

Similarly, the number of atoms outside the condensate (i.e., the depletion) is evaluated as

$$N' = \langle \delta c^\dagger \, \delta c \rangle = N \langle \delta \tilde{c}^\dagger \, \delta \tilde{c} \rangle = \frac{C_{3,3} + C_{4,4} - 1}{2}. \tag{38}$$

Figure 7 shows the steady-state number of particles outside the condensate for the parameter settings of the earlier plots. Notice that, on the right-hand side of the resonance, depletion is not plotted. In this regime, where the cavity heats atomic motion instead of cooling it, there is no steady-state condensate, and depletion grows in time exponentially. The steady-state depletion is analogous to the quantum depletion of the ground state of a nonideal Bose gas of atoms due to collisions. In the cavity case, the interaction between the atoms is provided by the collective coupling to the photon field. However, this depletion scales completely differently than that caused by s-wave scattering and is strongly influenced by the presence of the resonance. The diffusion of atoms out of the condensate can also be interpreted as a quantum

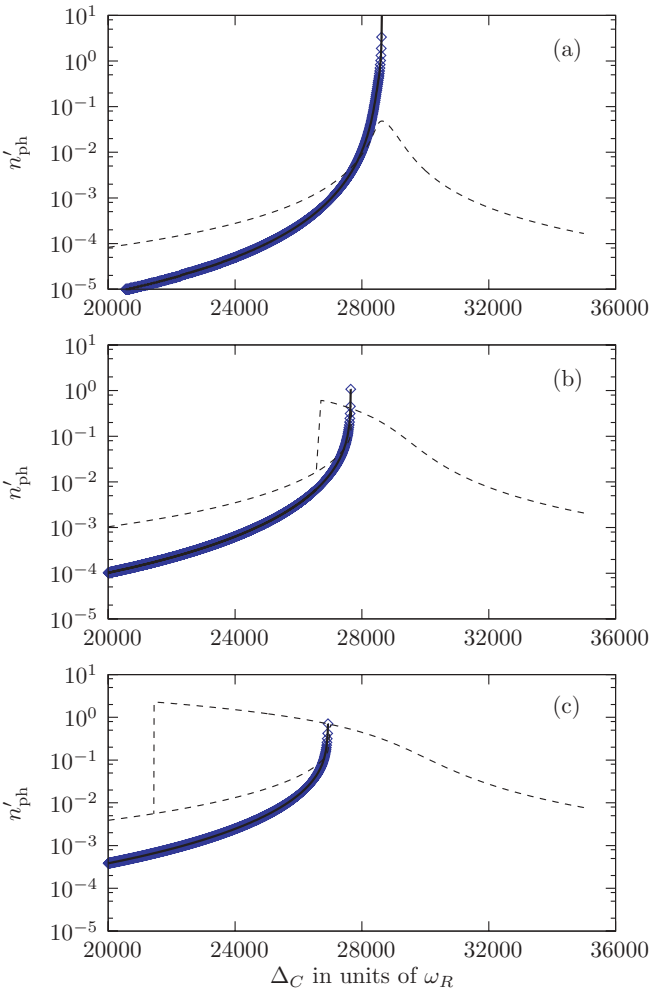

FIG. 6. (Color online) The nonclassical part of the photon number vs the cavity detuning of the optomechanical model. For reference we have also plotted the mean-field solution, $|\alpha_{\rm ss}|^2$, with a dashed line. All parameters are the same as for Fig. 2.

measurement-induced back-action process which stems from the dispersive atom-light interaction [5,19] and occurs even in phase contrast imaging of a condensate where the photon field is propagating in free space [46,47]. In a recent paper [18], we have shown that the depletion has a large steady-state value even in the limit of vanishing interaction strength U_0. For a fixed large detuning, $\Delta_C \gg \kappa, NU_0$, the amount of noncondensed atoms was estimated by Δ_C/ω_R and is connected to the ratio of the photon energy and the energy of motional excitations. In Fig. 7 the detuning is a variable and the above condition is not fulfilled. However, far from resonance, the same ratio determines the depletion with the effective photon energy given by the detuning δ_C.

The amount of entanglement between the atomic motional and photonic degrees of freedom can also be calculated with the help of the correlation function, assuming that the state of the system is a Gaussian one. The logarithmic negativity, $E_{\mathcal{N}}$, is a useful measure of entanglement in our case, since it can be directly calculated with the help of correlation matrix (35):

$$E_{\mathcal{N}} = \max(0, -\ln 2\eta^-), \tag{39a}$$

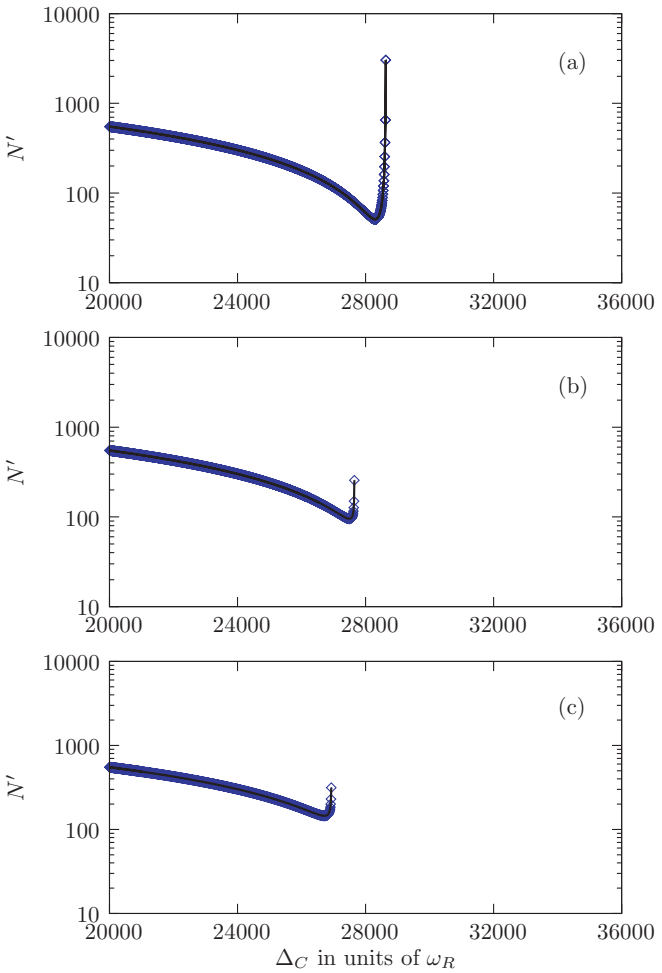

FIG. 7. (Color online) The depletion of the condensate vs the cavity detuning of the optomechanical model. All parameters are the same as for Fig. 2.

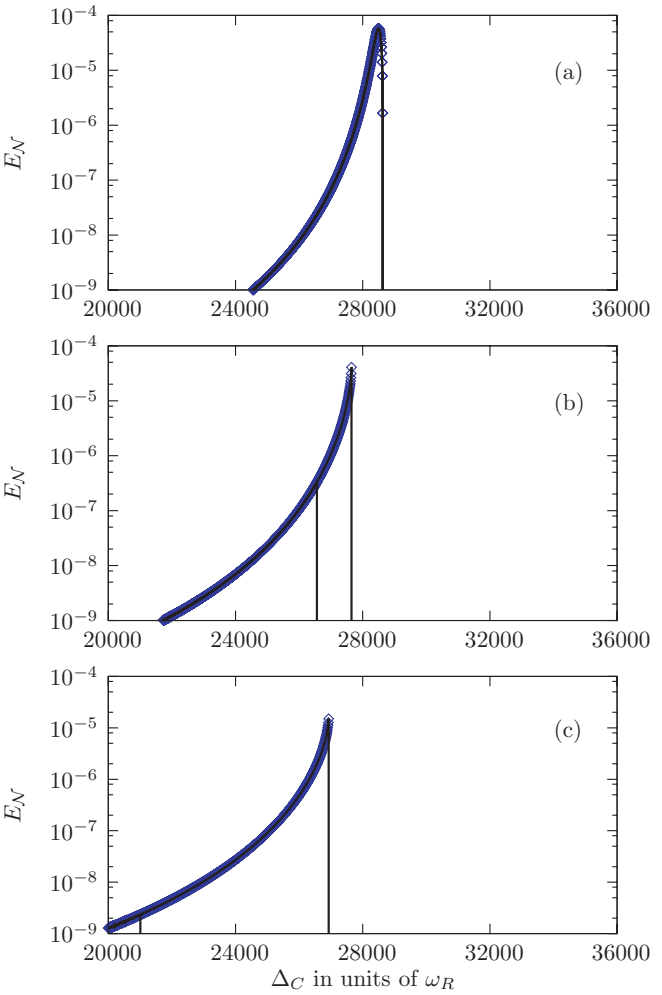

FIG. 8. (Color online) The logarithmic negativity of the condensate vs the cavity detuning of the optomechanical model. All parameters are the same as for Fig. 2.

where

$$\eta^- = 2^{-1/2}\sqrt{\Sigma(\mathbf{C}) - \sqrt{\Sigma(\mathbf{C})^2 - 4\det\mathbf{C}}} \tag{39b}$$

is the smaller symplectic eigenvalue of the two-mode Gaussian state, with $\Sigma(\mathbf{C}) = \det\mathbf{P} + \det\mathbf{A} - 2\det\mathbf{X}$. The state is an entangled state if and only if $E_{\mathcal{N}} \neq 0$. The larger the logarithmic negativity, the larger the entanglement between the atomic motion and the photonic degree.

Figure 8 shows the steady-state value of the logarithmic negativity, $E_{\mathcal{N}}$, as a function of Δ_C for the three parameter settings of Fig. 2. These results hold only for the cooling solution. In the heating regime, where there is no steady state, the entanglement between the photonic mode and the atomic motion also grows with time. The logarithmic negativity takes very small values in the whole range of the presented parameters except for a very small region around the instability. Apart from this narrow region, the entanglement is small even compared to the values of other optomechanical systems [17]. The smallness of the entanglement might be attributed to the big difference between the occupation numbers of the photonic and atomic modes or, equivalently, to the large difference in the effective energies of the decoupled subsystems. To reach higher values of entanglement, either the time scales of the photonic and atomic degrees of freedom should be closer to each other, or a much stronger driving is needed to attain high photon numbers.

IV. DISCUSSION

In this paper we have investigated the one-dimensional dynamics of a Bose-Einstein condensate inside a driven optical cavity. As the dispersive atom-photon interaction couples the atomic motion to the dynamics of the photonic field in a nonlinear way, strong correlations can appear. The strength of this coupling is inversely proportional to the detuning of the pump frequency from the atomic transition; therefore, it can be tuned in experimental implementations. We recited and analyzed the mapping of the original system to a two-mode effective model in which only the two highest populated one-particle states are kept from a plane-wave expansion of the atomic motion [3–5]. By solving the coupled Gross-Pitaevskii equations it was possible to reproduce the bistable behavior caused by the nonlinear coupling [1,4,25] and to provide a phase diagram of the system, partitioning the whole parameter space into regions with full dynamical stability of the

mean-field solution (the cooling region), to a region with a dynamical instability attributed to cavity heating, and to a region where both stable and unstable solutions can exist. We have compared the mean-field solution and the fluctuation spectrum of the optomechanical model to that of the model not restricted to the first two highly occupied modes. In the cavity heating region, the unstable polariton mode can have a positive imaginary part on the order of a kilohertz, giving an evaporation rate of the Bose-Einstein condensate in milliseconds. Such a time scale is within experimental reach.

The dispersive atom-photon interaction not only causes cavity cooling or cavity heating but also alters the statistics of the constituent subsystems. In the framework of the optomechanical model, second-order correlations were also investigated between the radiation field of the cavity and the motional mode of the Bose-Einstein condensate in the cavity cooling regime. Significant contributions to the photon and particle numbers were found, beyond that of the mean field. The strong depletion of the condensate shows some analogy with the excess noise in lasers [48,49], which was already discussed in our previous work [18]. It is interesting, however, that the huge nonclassical contribution in the autocorrelation of the photonic and atomic operators does not manifest in the entanglement of these variables. The lack of entanglement can be attributed to the big difference of the occupation of these modes. While the atom number was assumed to be on the order of 10^5, the photon number ranged on the order of unity.

The experimental progress in combining cavity quantum-electrodynamical systems with ultracold atoms promises an interesting playground to test the manifestation of light-matter interactions on the mesoscopic scale. In such systems both the radiation and the atomic part are dynamical entities. The better understanding of their interplay can have an impact not just on our knowledge of nonequilibrium systems, but also on implementations of quantum information processing devices or quantum simulators of other systems.

ACKNOWLEDGMENTS

The authors are grateful to András Vukics, Claudiu Genes, and Helmut Ritsch for useful discussions. We acknowledge funding from the National Scientific Fund of Hungary (Grant No. NF68736 and No. T077629) and from the National Office for Research and Technology (ERC_HU_09 OPTOMECH). G. Sz. acknowledges Spanish MEC projects TOQATA (FIS2008-00784), QOIT (Consolider Ingenio 2010), ERC Advanced Grant QUAGATUA, and EU STREP NAMEQUAM.

[1] F. Brennecke, T. Donner, S. Ritter, T. Bourdel, M. Köhl, and T. Esslinger, Nature **450**, 268 (2007).
[2] Y. Colombe, T. Steinmetz, G. Dubois, F. Linke, D. Hunger, and J. Reichel, Nature **450**, 272 (2007).
[3] F. Brennecke, S. Ritter, T. Donner, and T. Esslinger, Science **322**, 235 (2008).
[4] S. Ritter, F. Brennecke, K. Baumann, T. Donner, C. Guerlin, and T. Esslinger, Appl. Phys. B **95**, 213 (2009).
[5] K. W. Murch, K. L. Moore, S. Gupta, and D. M. Stamper-Kurn, Nature Phys. **4**, 561 (2008).
[6] S. Gupta, K. L. Moore, K. W. Murch, and D. M. Stamper-Kurn, Phys. Rev. Lett. **99**, 213601 (2007).
[7] J. Klinner, M. Lindholdt, B. Nagorny, and A. Hemmerich, Phys. Rev. Lett. **96**, 023002 (2006).
[8] S. Slama, G. Krenz, S. Bux, C. Zimmermann, and P. W. Courteille, Phys. Rev. A **75**, 063620 (2007).
[9] I. B. Mekhov, C. Maschler, and H. Ritsch, Phys. Rev. Lett. **98**, 100402 (2007).
[10] I. B. Mekhov and H. Ritsch, Phys. Rev. Lett. **102**, 020403 (2009).
[11] I. B. Mekhov and H. Ritsch, Phys. Rev. A **80**, 013604 (2009).
[12] W. Chen, D. Meiser, and P. Meystre, Phys. Rev. A **75**, 023812 (2007).
[13] W. Chen and P. Meystre, Phys. Rev. A **79**, 043801 (2009).
[14] F. Marquardt and S. M. Girvin, Physics **2**, 40 (2009).
[15] C. K. Law, Phys. Rev. A **51**, 2537 (1995).
[16] D. Vitali, S. Gigan, A. Ferreira, H. R. Böhm, P. Tombesi, A. Guerreiro, V. Vedral, A. Zeilinger, and M. Aspelmeyer, Phys. Rev. Lett. **98**, 030405 (2007).
[17] C. Genes, A. Mari, P. Tombesi, and D. Vitali, Phys. Rev. A **78**, 032316 (2008).
[18] G. Szirmai, D. Nagy, and P. Domokos, Phys. Rev. Lett. **102**, 080401 (2009).
[19] D. Nagy, P. Domokos, A. Vukics, and H. Ritsch, Eur. Phys. J. D **55**, 659 (2009).
[20] P. Horak, S. M. Barnett, and H. Ritsch, Phys. Rev. A **61**, 033609 (2000).
[21] P. Horak and H. Ritsch, Phys. Rev. A **63**, 023603 (2001).
[22] D. Nagy, G. Szirmai, and P. Domokos, Eur. Phys. J. D **48**, 127 (2008).
[23] J. M. Zhang, W. M. Liu, and D. L. Zhou, Phys. Rev. A **77**, 033620 (2008).
[24] J. M. Zhang, W. M. Liu, and D. L. Zhou, Phys. Rev. A **78**, 043618 (2008).
[25] J. M. Zhang, F. C. Cui, D. L. Zhou, and W. M. Liu, Phys. Rev. A **79**, 033401 (2009).
[26] S. Gopalakrishnan, B. L. Lev, and P. M. Goldbart, Nature Phys. **5**, 845 (2009).
[27] M. G. Moore, O. Zobay, and P. Meystre, Phys. Rev. A **60**, 1491 (1999).
[28] L. Fallani, C. Fort, N. Piovella, M. Cola, F. S. Cataliotti, M. Inguscio, and R. Bonifacio, Phys. Rev. A **71**, 033612 (2005).
[29] W. H. Louisell, *Quantum Statistical Properties of Radiation* (Wiley, New York, 1973).
[30] F. Marquardt, J. G. E. Harris, and S. M. Girvin, Phys. Rev. Lett. **96**, 103901 (2006).
[31] Y. Castin, in *Coherent Atomic Matter Waves, Lecture Notes of Les Houches Summer School*, edited by R. Kaiser, C. Westbrook, and F. David (EDP Sciences and Springer-Verlag, 2001), pp. 1–136.
[32] C. Maschler, I. B. Mekhov, and H. Ritsch, Eur. Phys. J. D **46**, 545 (2008).
[33] A. Vukics, C. Maschler, and H. Ritsch, New J. Phys. **9**, 255 (2007).

[34] A. Vukics, W. Niedenzu, and H. Ritsch, Phys. Rev. A **79**, 013828 (2009).
[35] J. Larson, S. Fernandez-Vidal, G. Morigi, and M. Lewenstein, New J. Phys. **10**, 045002 (2008).
[36] J. Larson, B. Damski, G. Morigi, and M. Lewenstein, Phys. Rev. Lett. **100**, 050401 (2008).
[37] H. Zoubi and H. Ritsch, Phys. Rev. A **80**, 053608 (2009).
[38] D. S. Goldbaum, K. Zhang, and P. Meystre, e-print arXiv:0911.3234 (2009).
[39] P. Horak and H. Ritsch, Phys. Rev. A **64**, 033422 (2001).
[40] S. A. Gardiner, K. M. Gheri, and P. Zoller, Phys. Rev. A **63**, 051603(R) (2001).
[41] P. Horak, G. Hechenblaikner, K. M. Gheri, H. Stecher, and H. Ritsch, Phys. Rev. Lett. **79**, 4974 (1997).
[42] P. Maunz, T. Puppe, I. Schuster, N. Syassen, P. W. H. Pinkse, and G. Rempe, Nature **428**, 50 (2004).
[43] S. Nussmann, K. Murr, M. Hijlkema, B. Weber, A. Kuhn, and G. Rempe, Nature Phys. **1**, 122 (2005).
[44] A. Vukics, J. Janszky, and P. Domokos, J. Phys. B **38**, 1453 (2005).
[45] A. Vukics and P. Domokos, Phys. Rev. A **72**, 031401(R) (2005).
[46] U. Leonhardt, T. Kiss, and P. Piwnicki, Eur. Phys. J. D **7**, 413 (1999).
[47] D. A. R. Dalvit, J. Dziarmaga, and R. Onofrio, Phys. Rev. A **65**, 053604 (2002).
[48] F. Papoff, G. D'Alessandro, and G. L. Oppo, Phys. Rev. Lett. **100**, 123905 (2008).
[49] G. D'Alessandro and F. Papoff, Phys. Rev. A **80**, 023804 (2009).